# Coherent pion production by neutrinos

E. A. Paschos[*] and Dario Schalla[†]

*Department of Physics, TU Dortmund, D-44221 Dortmund, Germany*

In this paper we present quantitative results for coherent pion production by neutrinos scattered off nuclei within the framework developed by Gounaris, Kartavtsev, and Paschos. The method is based on partially conserved axial-vector current and uses helicity cross sections for the scattering of weak gauge bosons on nuclei. The process relies on experimental data for elastic pion-nucleus scattering. A detailed analysis of the differential and integrated cross sections is presented for neutral and charged currents, with special emphasis on the regions of integrations. The results are extended to energies of 10.0 GeV and are compared with experimental data.

## I. INTRODUCTION

The process of coherent pion production by neutrinos is one of the important reactions that occur in neutrino oscillation experiments. It dominates at very low momentum transfers of the leptons and in the forward direction which may help to monitor the flux of the beam and will help to estimate backgrounds. For instance in the oscillation of $\nu_\mu$ into $\nu_e$ one searches in the far-away detector the reaction $\nu_e N \rightarrow e^- X$ and coherent production of $\pi^0$'s produces a background. For this reason there are new theoretical articles and experimental measurements dealing with this process.

The neutral and charged current reactions are

$$\nu_\mu(k)N(p) \rightarrow \nu_\mu(k')N(p')\pi^0(p_\pi) \qquad (1)$$

$$\nu_\mu(k)N(p) \rightarrow \mu^-(k')N(p')\pi^+(p_\pi), \qquad (2)$$

where $N$ is a nucleus with mass $M$. For the process we use variables in the rest frame of the nucleus with $q = k - k'$, $Q^2 = -q^2$, $\nu = E - E'$, $E = k_0$, $E' = k'_0$, and $t = (q - p_\pi)^2$. In the early experiments [1,2] coherent production of pions was defined as the process where the nucleus does not break up or alters its quantum numbers during the process.

Because of the isospin structure of the charged and neutral currents, the charged cross section is at high energies, approximately twice as big as the neutral one. At low energies differences arise from the nonvanishing mass of the outgoing lepton and the Cabibbo-Kabayashi-Maskawa (CKM) matrix element in the charged current case. Hence it is sufficient to concentrate on the charged current reaction within the theory. Its Feynman diagram is shown in Fig. 1.

Our calculation [3] is based on two basic facts:

(1) Coherent production of pions is the process where the 4-momentum-transfer squared between the cur-

rent and the produced pion is small so the nucleus remains intact. The minimum value is given to a good approximation by

$$|t_{\min}| = \left(\frac{Q^2 + m_\pi^2}{2\nu}\right)^2 \qquad (3)$$

and is achieved for $\nu M \gg Q^2$ with $M$ the mass of the nucleus. The important experimental region will turn out to be $Q^2 < 0.1$ GeV$^2$. We remind the reader that, neglecting the nucleus recoil energy, $t$ is calculated as [4]

$$|t| = \left[\sum_{\mu,\pi} p_i^\perp\right]^2 + \left[\sum_{\mu,\pi}(E_i - p_i^{\parallel})\right]^2. \qquad (4)$$

(2) In this region, the dominant component of the leptonic current has helicity zero, i.e., $\epsilon_\mu(\lambda = 0)$ defined in Eq. (9) below. The domain $\nu M \gg Q^2$, $Q^2 = $ (a few)$m_\pi^2$, and $\nu^2 \gg Q^2$ [see Eq. (27)] is the region where partially conserved axial-vector current (PCAC) is valid and it has been shown that the dominant amplitude is determined by chiral symmetry. In fact when we write the amplitude for the subprocess $WN \rightarrow N\pi$ as the sum

$$\text{pion pole} + \mathcal{R}_\mu$$

with $\mathcal{R}_\mu$ the remainder, the symmetry determines

$$q_\mu \mathcal{R}^\mu = -f_\pi\sqrt{2}T(\pi^+ N \rightarrow \pi^+ N), \qquad (5)$$
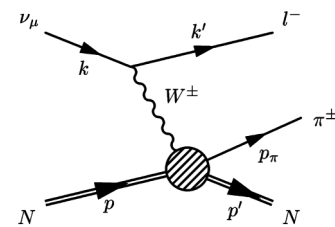


FIG. 1. Feynman diagram of the charged current reaction.

[*]paschos@physik.uni-dortmund.de
[†]dario.schalla@tu-dortmund.de

which is exactly the term that the zero helicity polarization selects and makes it dominant. In this picture the weak current converts the axial current into the pion field and the matrix element between the states is a smooth function. We shall quantify these results in the following sections.

This approach has many advantages:

(1) It avoids discussing what happens within the nucleus since it will use $\pi N$ elastic scattering data. In this sense it incorporates the pion-nucleus diffractive peak into the neutrino scattering.

(2) It is applicable at low and high energies, provided that some required kinematic cuts are made.

(3) It includes the lepton mass exactly and quantifies various approximations.

The purpose of this article is to quantify the results with numerical calculations. There are other articles on this topic [5–10]. One among them follows the same approach [5]. A very different approach describes coherent pion production at very low energies as the excitation of the $\Delta$-resonance and includes modifications through nuclear medium effects demanding that the nucleus remains in its ground state for coherent scattering [6–10].

## II. THEORY REVISITED

The theoretical background of this paper is the same as in [3]. For completeness we repeat its main features. The invariant matrix element of the charged current reaction is

$$\mathcal{M} = -\frac{G_F V_{ud}}{\sqrt{2}} j_\mu \langle \pi N | J^\mu | N \rangle, \quad (6)$$

where $G_F$ is the Fermi coupling constant and $V_{ud}$ the CKM matrix element. The leptonic current is expressed in a straightforward way

$$j_\mu = \bar{u}(k') \gamma_\mu (1 - \gamma_5) u(k), \quad (7)$$

whereas the hadronic matrix element will be treated below.

The leptonic current is decomposed into the basis of the four polarization vectors of the exchange boson. Select the 3-momentum of $q_\mu$ along the $z$ axis and define the basis of polarization vectors

$$\epsilon_\mu^l = \frac{q_\mu}{\sqrt{Q^2}} = \frac{1}{\sqrt{Q^2}} \begin{pmatrix} \nu \\ 0 \\ 0 \\ |\vec{q}| \end{pmatrix} \quad (8)$$

$$\epsilon_\mu(\lambda \pm 1) = \frac{1}{\sqrt{2}} \begin{pmatrix} 0 \\ 1 \\ \pm i \\ 0 \end{pmatrix}, \qquad \epsilon_\mu(\lambda = 0) = \frac{1}{\sqrt{Q^2}} \begin{pmatrix} |\vec{q}| \\ 0 \\ 0 \\ \nu \end{pmatrix}. \quad (9)$$

Note that they differ from the original paper [3] by their normalization factors. This has been taken into account in

the following formulas but does not change the results. The polarization vectors satisfy the completeness relation

$$\sum_{\lambda=0,\pm 1} (-1)^\lambda \epsilon^\mu(\lambda) \epsilon^{\nu*}(\lambda) - \epsilon_l^\mu \epsilon_l^\nu = g^{\mu\nu}. \quad (10)$$

In the cross sections the leptonic tensor appears

$$T_{\mu\nu} = 8(k_\mu k'_\nu + k_\nu k'_\mu - g_{\mu\nu} k \cdot k') + 8i\varepsilon_{\mu\alpha\nu\beta} k^\alpha k'^\beta \quad (11)$$

$$= \sum_{JJ'} L_{JJ'} \epsilon_\mu(J) \epsilon_\nu^*(J') \quad (12)$$

with the indices running over the four polarizations. Numerical studies in Ref. [3] have shown that the transverse polarizations, i.e., right- and left-handed cross sections are smaller in coherent scattering and they will be omitted.

From Eq. (12) we obtain the relevant matrix elements:

$$L_{00} = 4 \frac{[Q^2(2E_\nu - \nu) - \nu m_\mu^2]^2}{Q^2(Q^2 + \nu^2)} - 4(Q^2 + m_\mu^2) \quad (13)$$

$$L_{l0} = 4m_\mu^2 \frac{Q^2(2E_\nu - \nu) - \nu m_\mu^2}{Q^2 \sqrt{Q^2 + \nu^2}} \quad (14)$$

$$L_{ll} = 4m_\mu^2 \left(1 + \frac{m_\mu^2}{Q^2}\right). \quad (15)$$

Here the mass of the lepton in the final state is explicit and will be kept throughout the calculation. We also use later $\tilde{L}_{ij}$ as in Ref. [3] and the relation between them is $\tilde{L}_{ij} = \frac{1}{2} L_{ij}$.

It is now possible to write the spin-averaged matrix element as

$$\overline{|\mathcal{M}|^2} = \frac{G_F^2 |V_{ud}|^2}{2} \{ L_{00} |J_\mu \epsilon_0^\mu|^2 + L_{ll} |J_\mu \epsilon_l^\mu|^2 + 2L_{l0} (J_\mu \epsilon_l^\mu)(J_\mu \epsilon_0^\mu)^* \}. \quad (16)$$

As mentioned in the introduction the divergence of the matrix element is determined by PCAC. The matrix element of the axial current can be written as a sum of the pion pole and the remaining contribution

$$-i\mathcal{A}_\mu^+ = \frac{\sqrt{2} f_\pi q_\mu}{Q^2 + m_\pi^2} T(\pi^+ N \to \pi^+ N) - \mathcal{R}_\mu, \quad (17)$$

where $T(\pi^+ N \to \pi^+ N)$ is the elastic scattering on a nucleus and $\mathcal{R}_\mu$ is a smooth function which includes all other contributions. The PCAC relation gives

$$-iq^\mu \mathcal{A}_\mu^+ = \frac{\sqrt{2} f_\pi m_\pi^2}{Q^2 + m_\pi^2} T(\pi^+ N \to \pi^+ N). \quad (18)$$

Combining the two equations one obtains

$$q^\mu \mathcal{R}_\mu = -\sqrt{2} f_\pi T(\pi^+ N \to \pi^+ N). \qquad (19)$$

With these relations one is also able to calculate all matrix elements in Eq. (16) because

$$\epsilon_\mu^l \mathcal{A}^{\mu+} = -i \frac{q^\mu A_\mu^+}{\sqrt{Q^2}} \qquad (20)$$

is given by Eq. (18) and is proportional to $m_\pi^2$.

The matrix element for helicity zero is calculated in the following way. From the property $\epsilon^\mu(\lambda = 0) q_\mu = 0$ it follows that the inner product of the pion pole with the helicity zero polarization vanishes. The remaining term is now estimated

$$\epsilon^\mu(\lambda = 0)\mathcal{R}_\mu = \frac{q^\mu}{\sqrt{Q^2}} \mathcal{R}_\mu + \mathcal{O}\left(\frac{\sqrt{Q^2}}{\nu}\right)$$

$$= -\frac{\sqrt{2} f_\pi}{\sqrt{Q^2}} T(\pi^+ N \to \pi^+ N) + \mathcal{O}\left(\frac{\sqrt{Q^2}}{\nu}\right).$$

$$(21)$$

Thus the matrix elements for both polarizations are estimated.

We write next the triple differential cross section as

$$\frac{d\sigma_{CC}}{dQ^2 d\nu dt} = \frac{G_F^2 |V_{ud}|^2}{2(2\pi)^2} \frac{\nu}{E_\nu^2} \frac{f_\pi^2}{Q^2} \left\{ \tilde{L}_{00} + \tilde{L}_{ll} \left(\frac{m_\pi^2}{Q^2 + m_\pi^2}\right)^2 \right.$$

$$\left. + 2\tilde{L}_{l0} \frac{m_\pi^2}{Q^2 + m_\pi^2} \right\} \frac{d\sigma_\pi}{dt}, \qquad (22)$$

where $\sigma_\pi$ is the elastic pion-nucleus cross section and where all muon mass terms have been kept in the calculation. As mentioned already, the right- and left-handed cross sections are small and have been neglected. Since they appear as positive additive terms, our estimate is a lower bound for the coherent cross section.

The corresponding neutral current cross section is

$$\frac{d\sigma_{NC}}{dQ^2 d\nu dt} = \frac{G_F^2}{4(2\pi)^2} \frac{\nu}{E_\nu^2} \frac{f_\pi^2}{Q^2} \tilde{L}_{00} \frac{d\sigma_\pi}{dt}. \qquad (23)$$

In this formula the muon mass in $\tilde{L}_{00}$ has to be set zero.

### III. METHODS OF INTEGRATION

The most detailed and convincing evidence for coherent scattering is the explicit observation of the triple differential cross sections in Eqs. (22) and (23). The characteristic signature is the sharp peak in the $t$ distributions which was the main feature in the original discovery and interpretation [1,2,11]. Subsequent and recent experiments integrate over the $t$ and other variables so that special attention must be given to the ranges of integration in order to ascertain that the model is still valid in these regions. In this article we shall integrate over data for $\pi^+ C^{12}$ elastic scattering.

TABLE I. Parameters of the elastic pion nucleus cross section model.

| $\nu$ (GeV) | $a$ (barn/GeV$^2$) | $b$ (GeV$^{-2}$) |
| --- | --- | --- |
| 0.210 | 28.526 | 159.657 |
| 0.228 | 28.659 | 147.986 |
| 0.260 | 32.012 | 129.022 |
| 0.290 | 27.162 | 101.910 |
| 0.320 | 23.600 | 90.824 |
| 0.340 | 22.734 | 90.660 |
| 0.370 | 19.000 | 83.814 |
| 0.400 | 17.924 | 84.590 |
| 0.420 | 14.594 | 73.256 |
| 0.766 | 3.759 | 49.459 |
| 0.864 | 4.172 | 58.149 |
| 0.942 | 3.649 | 56.197 |
| 1.046 | 3.523 | 53.497 |

We identify the incoming pion energy with the variable $\nu$ and integrate over experimental data for elastic pion-nucleus scattering [12–14]. We parametrized the cross section as follows:

$$\frac{d\sigma_\pi}{dt} = a \exp[-b|t|] \qquad (24)$$

and fitted the parameters $a$ and $b$ to the data. Their numerical values are given in Table I.

As in Ref. [3] we integrate first the variable $t$ over the range

$$\left(\frac{Q^2 + m_\pi^2}{2\nu}\right)^2 \le |t| \le \infty. \qquad (25)$$

The upper limit of integration should be the first diffractive minimum and has been extended to infinity because the numerical results are insensitive to values of the cross sections beyond the first diffractive minimum, the cross section being already too small. The other limit of integration is important at low energies and influences the $Q^2$ dependence. The integrated elastic pion-nucleus cross section

$$\sigma_\pi(Q^2, \nu) = \int_{t_{\min}}^\infty \frac{d\sigma_\pi}{dt} dt \qquad (26)$$

depends on $Q^2$ and $\nu$ and the results are shown in Fig. 2. In Ref. [3] the $\nu$ range was limited to 0.4 GeV and now we extend it to $\nu = 1.0$ GeV. The data have been extrapolated as constants in regions not covered by data. We observe again a sharp $Q^2$ dependence.

The integration over $\nu$ should respect the condition

$$\nu \gg \sqrt{Q^2} \qquad (27)$$

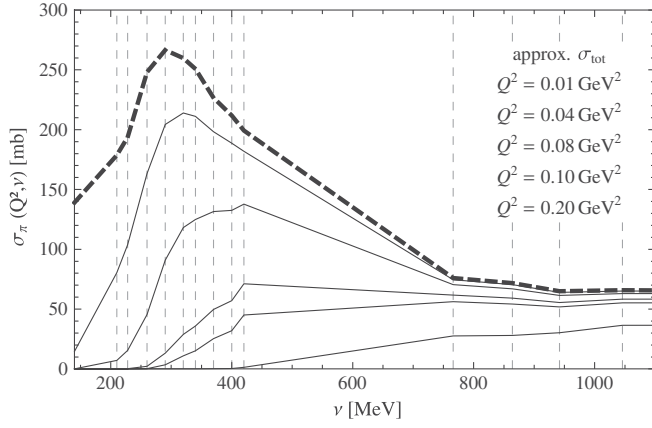so that the helicity $\lambda = 0$ polarization can be expanded to give

FIG. 2.   Integrated elastic pion-nucleus cross section for some momentum transfers.



FIG. 4 (color online).   Double-differential charged current cross section at $E_\nu = 10$ GeV. The lines represent different integration limits (see text).

$$\epsilon_\mu(\lambda = 0) \approx \frac{q_\mu}{\sqrt{Q^2}} + \mathcal{O}\left(\frac{\sqrt{Q^2}}{\nu}\right), \qquad (28)$$

which has been used in Eqs. (21)–(23). In order to test this condition we computed the double-differential cross section $\frac{d\sigma}{dQ^2 d\nu}$ over the entire range of $Q^2$ and $\nu$ using as input the curves in Fig. 2. The results are shown in Figs. 3 and 4 where we also include four curves. These four curves correspond to the kinematic regions defined in Table II.

In the earlier article [3] we used the variable $\xi$, which defined kinematic regions available in the experiments. It is a fortunate property of coherent scattering that the cross section peaks at low values of $Q^2$ and $\nu$. In fact the contribution to the integrated cross section from the region

$$0 < \nu < \sqrt{Q^2} \qquad (29)$$

is negligible. Our estimates are satisfied for $\nu > 1.5\sqrt{Q^2}$ where most of the cross section is located. One can also integrate over restricted regions of the phase space in order
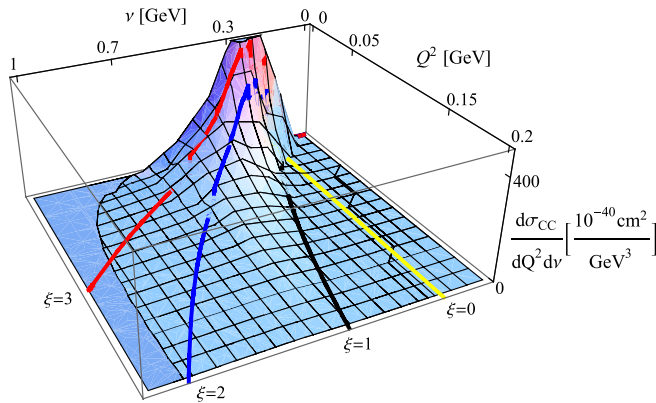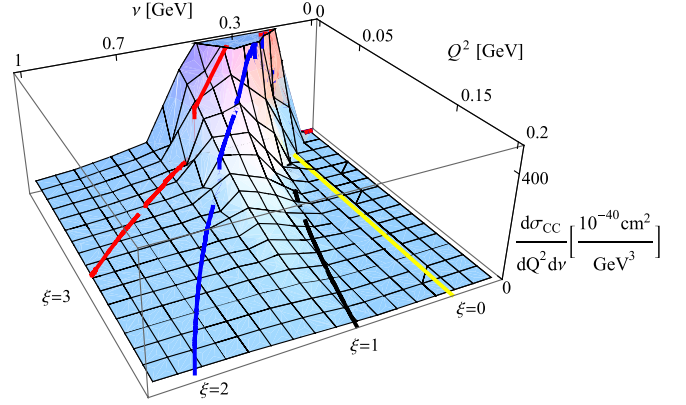
TABLE II.   Defining regions of phase space.

| Condition | Value of $\xi$ in Ref. [3] |
|---|---|
| $\nu = \nu_{\min}$ | $\xi = 0$ |
| $\nu = \sqrt{Q^2}$ | $\xi = 1$ |
| $\nu = 2\sqrt{Q^2}$ | $\xi = 2$ |
| $\nu = 3\sqrt{Q^2}$ | $\xi = 3$ |

to determine the fraction of the cross section in these regions.

The structure of the cross section in Fig. 3 also indicates the important regions of integration. To assure the validity of the approximation in Eq. (21) we integrate over the range

$$\max(\xi\sqrt{Q^2}, \nu_{\min}) < \nu < \nu_{\max}. \qquad (30)$$

The values for $\nu_{\min}$ and $\nu_{\max}$ are given in the appendix of Ref. [3].

The $Q^2$ integration is discussed later on. The lower limit of integration is given in Eq. (A8) of Ref. [3]. In the neutral current case it is zero.

We calculated the differential cross section $\frac{d\sigma}{dQ^2}$ for $E_\nu = 1$ GeV and four values for the lower limit of the energy $\nu$. The results are shown for neutral currents in Fig. 5 and for charged currents in Fig. 6. The four curves correspond to various cuts in the minimum value of the energy $\nu$, defined in Table II. We note that the cross section between $\nu_{\min} < \nu < \sqrt{Q^2}$ is negligibly small since the dashed curves for $\nu > \nu_{\min}$ coincide with the curves for $\nu > \sqrt{Q^2}$.

We repeated this calculation for various incident neutrino energies and the results are shown in Figs. 7 and 8 for neutral and charged currents, respectively. The interesting feature is that the cross section extends now to higher values of $Q^2$. Although the differential cross section is concentrated at low momentum transfers, for higher neu-
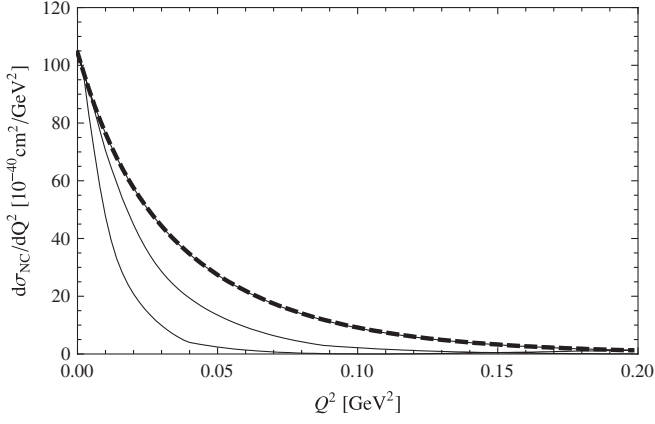


FIG. 3 (color online).   Double-differential charged current cross section at $E_\nu = 1$ GeV. The lines represent different integration limits (see text).

FIG. 5.   Differential neutral current cross section for $\xi = 1, 2, 3$ (top to bottom) and $\xi = 0$ (dashed) at $E_\nu = 1$ GeV.



FIG. 7.   Differential neutral current cross section for $\xi = 0$ at $E_\nu = 1, 5,$ and 10 GeV (bottom to top).

trino energies there is a tail that extends to larger values of $Q^2$ and must be taken into account in the integrated cross sections.

The neutral current cross section reaches a specific value at $Q^2 = 0$, the Adler point. It is estimated from our formulas (13) and (23) to give

$$\frac{d\sigma_{NC}}{dQ^2}\bigg|_{Q^2=0} = \frac{G_F^2 f_\pi^2}{2\pi^2} \int_{m_\pi}^{E_\nu} d\nu \, \sigma_\pi(\nu)\left\{\frac{1}{\nu} - \frac{1}{E_\nu}\right\} \quad (31)$$

$$= \frac{G_F^2 f_\pi^2}{2\pi^2} \langle \sigma_\pi \rangle \left\{\ln\frac{E_\nu}{m_\pi} + \frac{m_\pi}{E_\nu} - 1\right\}, \quad (32)$$

where $\langle \sigma_\pi \rangle$ is the weighted elastic pion-nucleus cross section. For $E_\nu = 1$ GeV the Adler point is about $112 \cdot 10^{-40} \frac{\text{cm}^2}{\text{GeV}^2}$ for $\langle \sigma_\pi \rangle \approx 165$ mb. This is a realistic average of the weighted hadronic cross section (see Fig. 2). A similar comparison for the charged current is more indirect because of the phase space effects introduced by the mass of the muon. For the charged current an integration over a
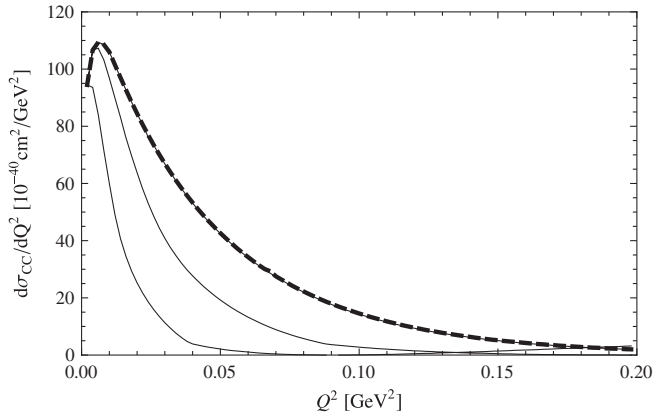
small region of $Q^2$ is more appropriate for comparison with experiments.

It is worth mentioning that for higher energies the turn-over of the differential cross section in the charged current case is less prominent and disappears, a property caused by the fact that the muon mass is negligible compared to the neutrino energy.

At higher neutrino energies bigger momentum transfers gain more importance. Figures 7 and 8 show the differential cross section of the neutral and charged current process, respectively, for $\xi = 0$. For higher energies the cross section is not limited within a small $Q^2$ region. Thus the $Q^2$ integration interval has to be extended to higher values.

## IV. INTEGRATED CROSS SECTION

The results in Fig. 8 indicate that the formulas we derived have a tail that extends to higher values of $Q^2$. However, at large values of $Q^2$ the nucleus breaks up and the scattering is not coherent. At the same time the PCAC approximation does not hold. Experimental groups separate the coherent events from other events by the absence



FIG. 6.   Differential charged current cross section for $\xi = 1, 2, 3$ (top to bottom) and $\xi = 0$ (dashed) at $E_\nu = 1$ GeV.
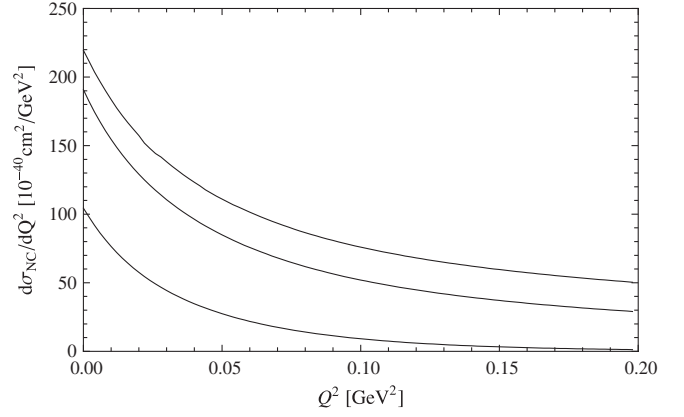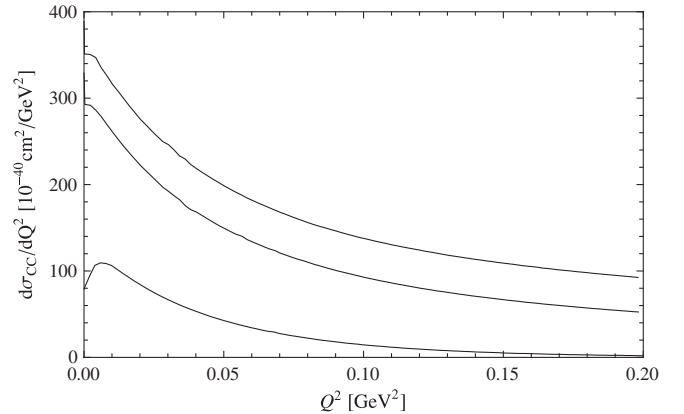


FIG. 8.   Differential charged current cross section for $\xi = 0$ at $E_\nu = 1, 5,$ and 10 GeV (bottom to top).
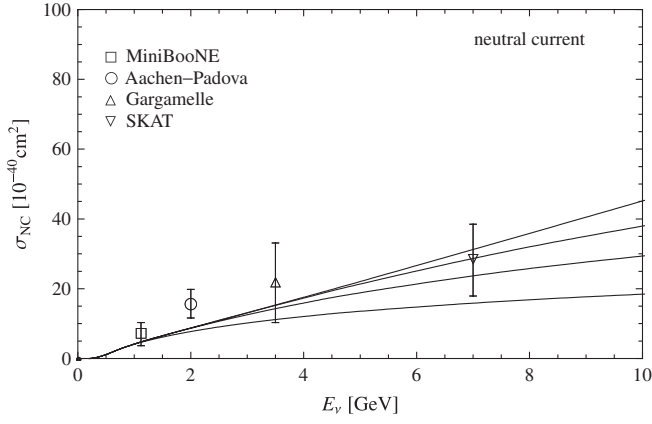
FIG. 9. Integrated neutral current cross section with $Q^2_{max} = 0.2, 0.5, 1.0$, and $4.0$ GeV$^2$ for $\xi = 0$ (bottom to top). See [1,17–19] for experimental data.



FIG. 10. Integrated charged current cross section with $Q^2_{max} = 0.2, 0.5, 1.0$, and $4.0$ GeV$^2$ for $\xi = 0$ (bottom to top). See [19–21] for experimental data.

of stubs in bubble chambers, a signature indicating that the nucleus does not break up. The BEBC Collaboration [15] found that the $Q^2$ values are lower for coherent events and do not extend beyond 2.0 GeV$^2$. These results suggest that a $Q^2_{max}$ must be introduced in the integration of the cross section or a phenomenological factor $(\frac{m_A^2}{Q^2+m_A^2})^2$ in order to provide a cutoff in the $Q^2$ dependence (see [16]). Fortunately, in the curves in Figs. 9 and 10, to be described below, the change between $Q^2 = 1$ and $4$ GeV$^2$ is relatively small.

In this work we calculate integrated coherent cross sections for various upper values of $Q^2_{max} = 0.2, 0.5, 1.0,$ and 4.0 GeV$^2$. The results are shown in Fig. 9 for neutral current and Fig. 10 for charged current reactions, where the effect of $Q^2_{max}$ is important.

For comparison we also included experimental results from several groups [1,17–21]. The experiments use different targets which we must rescale to the carbon target. Since the pion-nucleus cross section is a main input in this work we must rescale the results according to

$$\sigma_{carbon} = \sigma_{exp}\left(\frac{A_{carbon}}{A_{exp}}\right)^{2/3}, \qquad (33)$$

which has been established in pion-nucleus elastic scattering [22]. With this rescaling the agreement at higher energies prefers a $Q^2_{max}$ close to 1.0 GeV$^2$. For the energy of the neutrinos we use an average value from the neutrino flux.

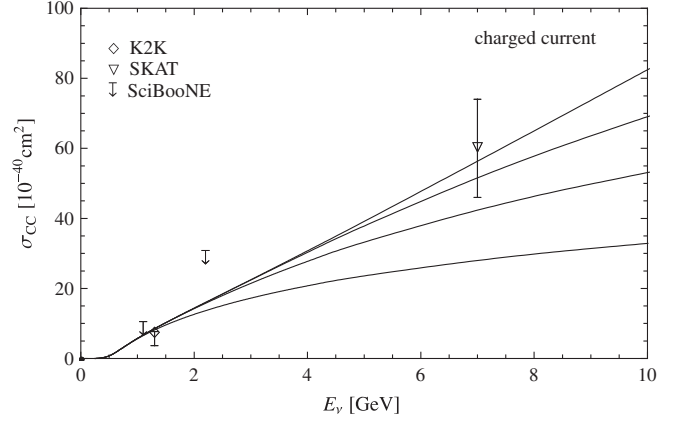There are two ways to account for the $Q^2$ dependence:

(1) Whenever possible, introduce an experimental cut-off to the coherent events where our model is valid.
(2) Integrate the cross sections on Eqs. (22) and (23) with a phenomenological factor $(\frac{m_A^2}{Q^2+m_A^2})^2$, introduced by other authors [11,16], which represents the effects of heavier vector mesons and treat $m_A$ as a parameter.

## V. SUMMARY

Neutrino-induced coherent pion production is described adequately by the method described in Ref. [3]. It is argued again that chiral symmetry relates coherent production of pions to the pion-nucleus elastic scattering in a general way, provided that $Q^2 \approx$ (a few) $\cdot m_\pi^2$.

Our formalism and results are close but not identical to a recent article [5], where the elastic pion-carbon data are now used as well, which reduces the earlier prediction [11]. We both use elastic pion-nucleus scattering data and the small differences arise from the handling of the experimental data and the limits of integrations.

Using pion-carbon scattering data we presented quantitative results for many cross sections. We emphasize that kinematic limits, as in Eq. (25) for $t$ and the maximum value of $Q^2$ in Figs. 7–10, are important. An overview of the double-differential cross section is shown in Figs. 3 and 4 showing the main features of the process. The calculation can be extended to higher energies when the value of $Q^2_{max}$ is better understood.

[1] H. Faissner *et al.*, Phys. Lett. **125B**, 230 (1983).
[2] P. Marage *et al.* (WA59), Phys. Lett. **140B**, 137 (1984).

[3] A. Kartavtsev, E. A. Paschos, and G. J. Gounaris, Phys. Rev. D **74**, 054007 (2006).

[4] P. Marage *et al.* (BEBC WA59 Collaboration), Z. Phys. C **43**, 523 (1989).

[5] C. Berger and L. M. Sehgal, Phys. Rev. D **79**, 053003 (2009).

[6] L. Alvarez-Ruso, L. S. Geng, S. Hirenzaki, and M. J. Vicente Vacas, Phys. Rev. C **75**, 055501 (2007).

[7] L. Alvarez-Ruso, L. S. Geng, and M. J. Vicente Vacas, Phys. Rev. C **76**, 068501 (2007).

[8] S. K. Singh, M. Sajjad Athar, and S. Ahmad, Phys. Rev. Lett. **96**, 241801 (2006).

[9] J. E. Amaro, E. Hernandez, J. Nieves, and M. Valverde, Phys. Rev. D **79**, 013002 (2009).

[10] S. X. Nakamura, T. Sato, T. S. H. Lee, B. Szczerbinska, and K. Kubodera, arXiv:0901.2366.

[11] D. Rein and L. M. Sehgal, Nucl. Phys. **B223**, 29 (1983).

[12] R. M. Edelstein, W. F. Baker, and J. Rainwater, Phys. Rev. **122**, 252 (1961).

[13] F. G. Binon *et al.* (CERN-IPN [Orsay] Collaboration), Nucl. Phys. **B17**, 168 (1970).

[14] T. Takahashi *et al.*, Phys. Rev. C **51**, 2542 (1995).

[15] P. Marage *et al.* (BEBC WA59 Collaboration), Z. Phys. C **31**, 191 (1986).

[16] A. A. Belkov and B. Z. Kopeliovich, Sov. J. Nucl. Phys. **46**, 499 (1987).

[17] J. L. Raaf, Fermilab Report No. fermilab-thesis-2005-20, 2005 (unpublished).

[18] E. Isiksal, D. Rein, and J. G. Morfin, Phys. Rev. Lett. **52**, 1096 (1984).

[19] H. J. Grabosch *et al.* (SKAT Collaboration), Z. Phys. C **31**, 203 (1986).

[20] M. Hasegawa *et al.* (K2K Collaboration), Phys. Rev. Lett. **95**, 252301 (2005).

[21] K. Hiraide *et al.* (SciBooNE Collaboration), Phys. Rev. D **78**, 112004 (2008).

[22] D. Ashery *et al.*, Phys. Rev. C **23**, 2173 (1981).